Rare Metal Materials and Engineering
Volume 53, Issue 1, January 2024
Available online at www.rmme.ac.cn

Science Press

Cite this article as: Xiao Haiyang, Lyu Guojian, Qiao Jichao. Dynamic Mechanical Behavior of In-situ $(Ti_{0.474}Zr_{0.34}Cu_{0.06}Be_{0.126})_{100-x}Fe_x$ (x=0, 2) Bulk Metallic Glass Composites[J]. Rare Metal Materials and Engineering, 2024, 53(01): 23-30. DOI: 10.12442/j.issn.1002-185X.E20230041.

ARTICLE

Dynamic Mechanical Behavior of In-situ $(Ti_{0.474}Zr_{0.34}Cu_{0.06}Be_{0.126})_{100-x}Fe_x$ (x=0, 2) Bulk Metallic Glass Composites

Xiao Haiyang, Lyu Guojian, Qiao Jichao

School of Mechanics, Civil Engineering and Architecture, Northwestern Polytechnical University, Xi'an 710072, China

Abstract: To understand the dynamic mechanical properties and thermodynamic stability of β-Ti phase-embedded Zr/Ti-based bulk metallic glass composites (BMGCs), $(Ti_{0.474}Zr_{0.34}Cu_{0.06}Be_{0.126})_{100-x}Fe_x$ (x=0, 2) BMGCs were prepared and investigated. Results show that by introducing Fe element, the stability of β-Ti phase is improved. An abnormal internal friction peak can be observed due to the precipitation of ω-Ti in the metastable β-Ti phase. Below the glass transition temperature T_g, both BMGCs show abnormal overshoot on storage modulus due to the coupling effect of phase transition and partial crystallization of amorphous matrix. This research provides information about the complex dynamic mechanical relaxation behavior of the in-situ metastable β-Ti BMGCs.

Key words: bulk metallic glass composites; dynamic mechanical analysis; physical aging; dynamic heterogeneity

Benefiting from the amorphous structure and defect absence, such as grain boundaries and dislocations, in the conventional alloys, bulk metallic glasses (BMGs) show superior mechanical properties[1]. Due to their long-range disorder atomic structure, BMGs have large elastic limit, superior yield strength, high hardness, excellent wear resistance, and superb formability[1–6]. Nevertheless, owing to the rapid development of highly-localized shear bands after loading at ambient temperature, BMGs usually show room temperature brittleness. The unstable propagation of shear bands leads to unpredictable failure, which restricts BMG applications as structural and functional engineering materials[7–10]. To hinder the rapid propagation of shear bands in BMGs and to promote the generation of multiple shear bands, the combination of BMGs and composite is commonly used to improve the ductility, toughness, and reliability[9]. Hence, different BMG composites (BMGCs) with ex-situ or in-situ introduction of the secondary crystalline phases have been explored[11–14].

Dual-phase composites of ex-situ BMGCs usually involve the addition of the secondary phases, which can effectively hinder the evolution of shear bands in micro-cracks and encourage the formation of multiple shear bands. The relevant composites include the fiber-reinforced[15] and particle-reinforced[16–17] BMGCs, according to the continuity of the secondary phases[18–20]. Although ex-situ phases are effective addition, in-situ crystalline phases are also widely considered because they can bear plastic deformation within the glassy matrix during melt solidification. The in-situ crystalline phases mainly include nanocrystallites, dendrites, and crystalline phases, which undergo the martensitic transformation during plastic deformation. The hard phases (metallic glass matrix) are surrounded by soft phases (crystalline phases), leading to extensive formation, interactions, and multiplication of shear bands[21]. Under the loading condition, the shear bands in the glass matrix bypass the crystalline phase, and then they are spilt into more shear bands[22] or the crystalline phases are under shear deformation[23–24]. Undoubtedly, the propagation of shear bands is hindered by the ductile phases, and excellent plasticity can be achieved consequently[25–26]. It is under debate that the dual-phase composites including secondary phases of high volume fraction should have metallic glass matrix or crystalline matrix or not. Although the crystalline phase has high volume fraction, the continuous metallic glass is considered to be the matrix. This character of BMGCs is quite different from that of other common

Received date: October 02, 2023
Foundation item: National Natural Science Foundation of China (51971178, 52271153); Natural Science Basic Research Plan for Distinguished Young Scholars in Shaanxi Province (2021JC-12); Fundamental Research Funds for the Central Universities (D5000220034)
Corresponding author: Lyu Guojian, Ph. D., Associate Professor, School of Mechanics, Civil Engineering and Architecture, Northwestern Polytechnical University, Xi'an 710072, P. R. China, E-mail: guojian.lyu@nwpu.edu.cn

composites with amorphous phases as reinforcements[27–28].

According to the secondary strengthening phases, in-situ BMGCs can be classified as β-type and B2-type composites, which contain β-Zr/Ti dendrites[13,25,29–31] and B2-CuZr/Ti particles[32–35], respectively. Among them, Ti-based BMGCs attract much attention because of their easy processing, excellent mechanical properties, low density, and high glass-forming ability, presenting great potential in processing and lightweight material applications[13,36–39]. However, the in-situ Ti/Zr-based BMGCs with stable β-Zr/Ti phases and without the deformation-induced phase transformation usually have work softening and necking behavior under tensile conditions[13,23]. Generally, the β-type BMGCs are developed by adding a large number of β-stabilizing elements (Nb, Mo) into the Ti/Zr-based BMGs, which are stable under plastic deformation[25]. The metastable β phases can be transformed to ω-Ti phase, which is induced by deformation or heating. Therefore, the Ti-based BMGCs exhibit high tensile plasticity and work-hardening behavior[26,40–41].

In this research, $(Ti_{0.474}Zr_{0.34}Cu_{0.06}Be_{0.126})_{100-x}Fe_x$ (x=0, 2, at%) BMGCs with metastable β-Ti dendrites embedded in the glassy matrix were used as target component. The dynamic mechanical behavior and structural relaxation of these two BMGCs were investigated. Usually, in the Zr/Ti-based in-situ composites, superb tensile ductility and fracture toughness can be achieved by the addition of β-stabilizing elements (V, Nb, Ta), which can stabilize the dendrites in the high-temperature body-centered cubic (bcc) phase[42]. During the heating and annealing processes at sub-glass transition temperature T_g, the ω phase transformed from metastable β phase can be detected. The dynamic mechanical behavior of these BMGCs was measured by mechanical relaxation spectroscopy. The microstructure evolution of metastable β-Ti phase was investigated. In addition, the effects of physical aging and the thermal history on structural relaxation were discussed.

1 Experiment

The in-situ metallic glass matrix composites with composition of $(Ti_{0.474}Zr_{0.34}Cu_{0.06}Be_{0.126})_{100-x}Fe_x$ (x=0, 2, at%) were prepared by arc melting of high-purity Ti, Zr, Cu, Fe (purities over 99.9%), and Be (purity over 99.5%) materials under the high-purity Ar atmosphere. Each ingot was remelted four times to ensure the chemical homogeneity and then pour-cast into the water-cooled copper molds. Plate specimens with thickness of 5 mm, width of 20 mm, and length of about 35 mm were obtained. The $(Ti_{0.474}Zr_{0.34}Cu_{0.06}Be_{0.126})_{100}Fe_0$ and $(Ti_{0.474}Zr_{0.34}Cu_{0.06}Be_{0.126})_{98}Fe_2$ BMGCs were denoted as Fe0 and Fe2 specimens, respectively. The specimens with dimension of 1 mm×2 mm×30 mm were cut from the plate specimen for dynamic mechanical analysis (DMA) tests. DMA tests were conducted by commercial dynamic mechanical analyzer (DMA, TA Q800) under single cantilever mode.

The thermal properties of BMGC specimens were measured by differential scanning calorimetry (DSC, Perkin Elmer 8500) under the pure argon atmosphere with heating rate of 20 K/min. The phases of BMGCs were characterized by X-ray diffractometer (XRD, Burker D8 with Cu-Kα radiation).

2 Results and Discussion

2.1 Structural characterization

Fig. 1a shows XRD patterns of the as-cast $(Ti_{0.474}Zr_{0.34}Cu_{0.06}Be_{0.126})_{100-x}Fe_x$ (x=0, 2) BMGCs. The superimposed Bragg peaks and the broad diffraction peak correspond to the β-Ti crystalline and glassy phase, respectively. Only β-Ti phase can be detected in both specimens. Fig. 1b shows the characteristic temperatures in DSC curves of the as-cast $(Ti_{0.474}Zr_{0.34}Cu_{0.06}Be_{0.126})_{100-x}Fe_x$ (x=0, 2) BMGCs. The glass transition temperature (T_g) of Fe0 BMGC is 602 K. Before reaching the glass transition temperature, an exothermal peak, namely sub-T_g exothermal peak, can be observed at 517 K, which is caused by the structural change of β-Ti phase. In addition to the glass transition temperature (T_g=589 K), DSC curve of Fe2 BMGC has two crystallization temperatures (T_x) of 615 and 720 K, indicating the complex crystallization behavior. It is reported that two exothermal peaks correspond to two steps of the crystallization of Ti-based metallic glasses: the formation of quasi-crystalline phase and the formation of stable phase[43]. Considering that two phases have different thermal properties, they are inappropriate to represent the characteristic temperatures of BMGCs.

2.2 Dynamical mechanical properties

The storage modulus E' and loss modulus E'' are normalized by the unrelaxed modulus E_u, where E_u is assumed to equal E' at room temperature. Fig. 2 shows the normalized storage modulus E'/E_u and normalized loss modulus E''/E_u of

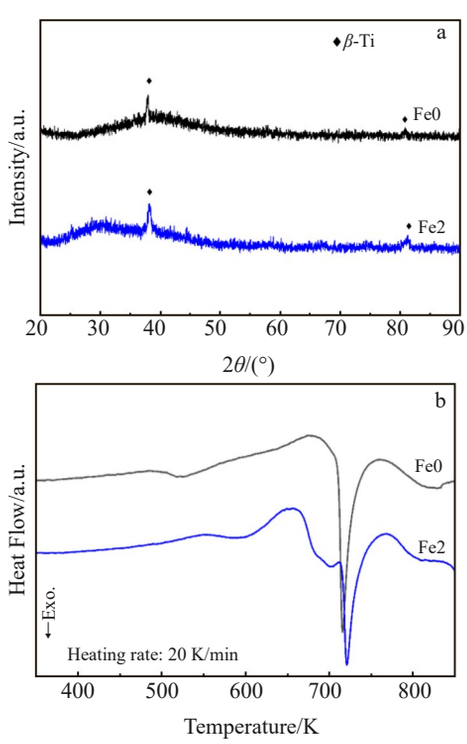

Fig. 1 XRD patterns (a) and DSC curves (b) of as-cast $(Ti_{0.474}Zr_{0.34}Cu_{0.06}Be_{0.126})_{100-x}Fe_x$ (x=0, 2) BMGCs

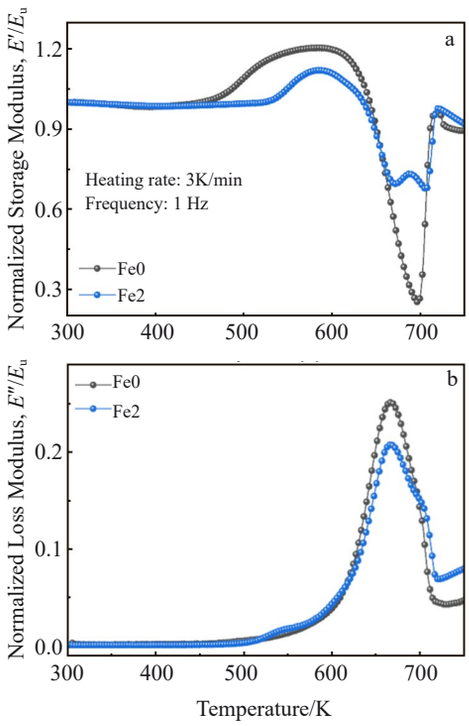

Fig.2 Normalized storage modulus E'/E_u (a) and normalized loss modulus E''/E_u (b) of $(Ti_{0.474}Zr_{0.34}Cu_{0.06}Be_{0.126})_{100-x}Fe_x$ (x=0, 2) BMGCs

Fe0 and Fe2 BMGCs at heating rate of 3 K/min and driving frequency of 1 Hz. Similar to the typical metallic glasses, three obvious temperature regions can be observed. Region I: at low temperature, the deformation of both BMGCs is controlled by elastic progress. E'/E_u is high and nearly constant; E''/E_u is very low and nearly 0. The normalized storage modulus is increased unconventionally with increasing the temperature to about 500 K and E'/E_u reaches the maximum value at approximately 600 K. This phenomenon of Ti-based metallic glass composites is attributed to the participation of ω-Ti phase[44–45]. Region II: with further increasing the temperature to 700 K, E''/E_u is decreased rapidly whereas E'/E_u is increased. The temperature correspond to the maximum E''/E_u is denoted as T_a, which is related to the dynamic glass transition and the cooperative motion of atoms. This temperature range is related to the supercooled liquid region (SLR) of metallic glasses. Region III: the normalized storage modulus E'/E_u is further increased with increasing the temperature due to the occurrence of crystallization.

As shown in Fig.2a, in the region I, the E'/E_u increment of Fe2 BMGC is slightly smaller than that of Fe0 BMGC. This is because after introducing 2at% Fe into the composite, the phase stability of the dendrites is improved. Because the volume fraction and morphology of β phase in Fe0 and Fe2 BMGCs are similar, the difference in storage modulus from 450 K to 625 K is mainly attributed to the difference in phase stability of β-Ti crystals. Compared with Fe0 BMGC, Fe2 BMGC has obvious shoulder curve on the loss modulus below the glass transition temperature, as shown in Fig. 2b. It is worth mentioning that the overshoot of storage modulus also starts at 550 K. Based on DSC results, an obvious exothermic peak can also be detected within the similar temperature range for the Fe2 BMGC, indicating that both the abnormal increase in storage modulus and the exothermic peak in DSC curve are caused by the same structural change in BMGCs. The large increase in storage modulus coupled with the increase in loss modulus implies the significant change of mechanical properties, such as the dendrite stiffness. This phenomenon is attributed to the phase transformation from metastable β-Ti phase to ω-Ti phase[44–46]. For metallic glasses, this shoulder phenomenon of loss modulus is related to the secondary Johari-Goldstein (JG) relaxation[47]. However, this shoulder phenomenon is also related to the precipitation of isothermal ω phase[44–46] with spacing group of P6/mm or $P\bar{3}m1$ in the metastable β-Ti dendrites[48]. In this research, it is believed that the abnormal increase in storage modulus of both BMGCs and the shoulder phenomenon in Fe2 BMGC are related to the precipitation of isothermal ω-Ti phase in metastable β-Ti dendrites. Normally, the phonon-softening mode $L\frac{2}{3}(1, 1, 1)$ exists in the bcc structure of metastable β-Ti[49], which forms ω phase during cooling process or causes the precipitation of isothermal ω phase during heating or annealing process. The metastability of β phase can be effectively evaluated by the precipitation in the β-type BMGCs.

The dynamic mechanical behavior of metallic glasses strongly depends on the testing frequencies[50]. Thus, the frequency was set as 0.3, 1, 2, and 8 Hz during the temperature scanning. Fig. 3 shows the normalized storage modulus E'/E_u and normalized loss modulus E''/E_u of Fe0 and Fe2 BMGCs under heating rate of 3 K/min and different frequencies. The curves at low temperature region (below 450 K) are nearly straight lines, which are similar to those of the conventional BMGCs. With increasing the frequency, the increment in E'/E_u value is almost unchanged, and the peak E''/E_u value slightly moves towards the high temperature region, which corresponds to the activated energy of moving units.

For Fe2 BMGC, both E'/E_u and E''/E_u curves have two peaks at about 650 K. With increasing the frequency, the first peak becomes less obvious whereas the second peak becomes more obvious, indicating that the first peak is insensitive to the frequency. This is a common phenomenon for the Ti-based BMGs and composites[51] instead of typical BMGs. The first peak presents the non-Arrhenius type and appears at almost the fixed temperature, i. e., it is not a pure relaxation peak. Therefore, the first crystallization of the glassy matrix corresponds to the first peak of curves, which decreases the loss modulus E''. Besides, the two peaks within the same temperature range of DSC curve correspond to two crystallization processes of Fe2 BMGC.

Fig. 4 shows the normalized storage modulus E'/E_u and normalized loss modulus E''/E_u of $(Ti_{0.474}Zr_{0.34}Cu_{0.06}Be_{0.126})_{100-x}$-

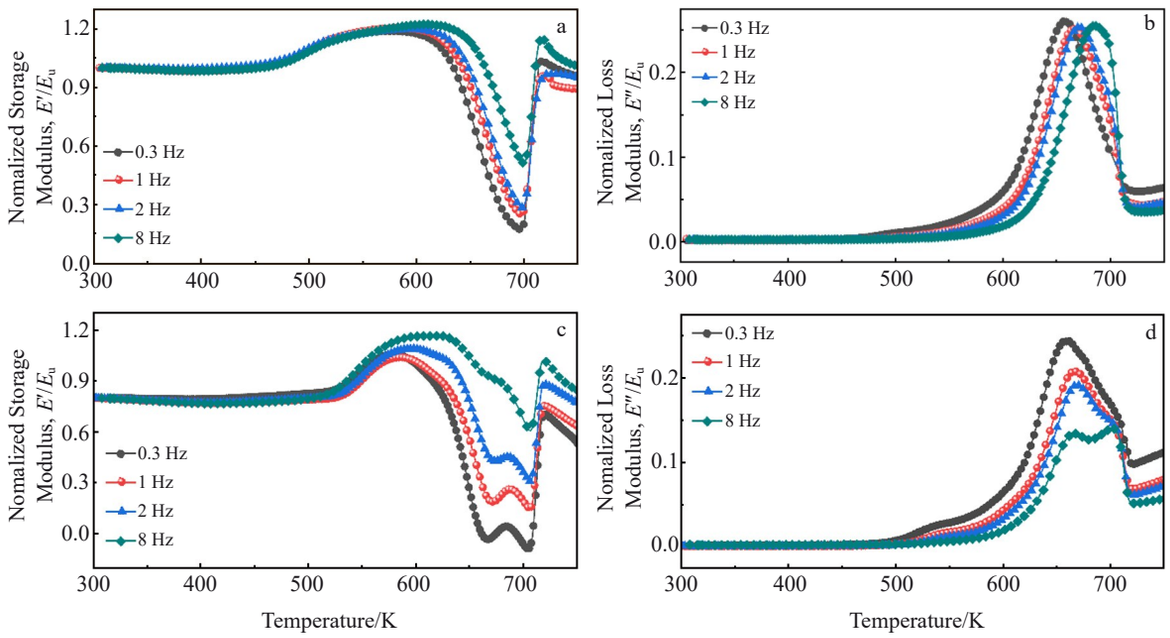

Fig.3 Normalized storage modulus E'/E_u (a, c) and normalized loss modulus E''/E_u (b, d) of Fe0 BMGC (a–b) and Fe2 BMGC (c–d) under heating rate of 3 K/min and different frequencies

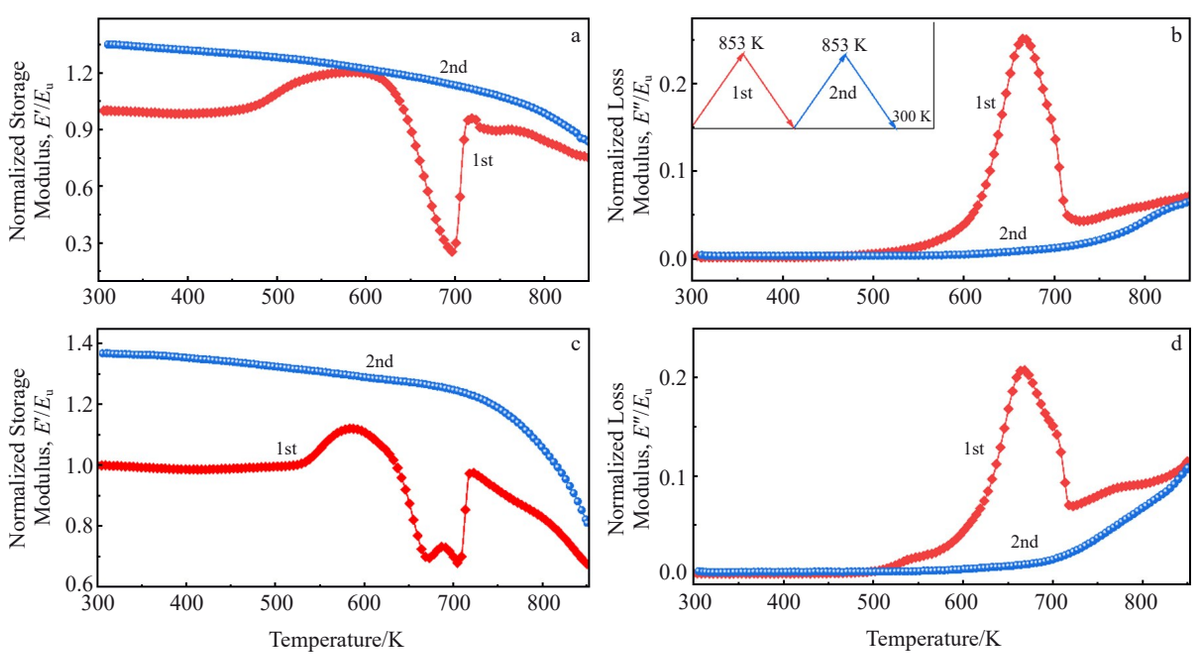

Fig.4 Normalized storage modulus E'/E_u (a, c) and normalized loss modulus E''/E_u (b, d) of Fe0 BMGC (a–b) and Fe2 BMGC (c–d) during continuous heating process under heating rate of 3 K/min and frequency of 1 Hz

Fe_x (x=0, 2) BMGCs during continuous heating process. The specimens were firstly heated to 853 K. After cooling to room temperature, the specimens were reheated to 853 K and then cooled to room temperature again. Because of the irreversible structural changes above the crystallization temperature induced by the first heating process, the reheating curves are quite different from those in the first heating process, which present the monotonous variation trend. In the reheating process, the normalized storage modulus increases by about 20% and the peak loss modulus disappears. Therefore, the crystallization of glassy matrix improves the elastic response, decreases the atomic mobility, and weakens the viscoelastic property of BMGCs.

2.3 Effects of physical aging on structural relaxation

Physical properties of glasses, such as density, enthalpy, and viscosity, slowly evolve at the temperature below the

glass transition temperature, which leads to the non-equilibrium glass materials[52]. This process is called as the physical aging, which happens in all types of glass materials and causes significant structural changes[53]. To investigate the non-equilibrium processes in metallic glasses, the time dependence on the physical properties should be investigated. For the metallic glasses and metallic glass composites, physical aging and thermal treatment can be used to tune the mechanical properties[44]. It is worth mentioning that during the annealing process below glass transition temperature, the metallic glasses present non-exponential variation process.

To study the effects of physical aging on the structural relaxation of $(Ti_{0.474}Zr_{0.34}Cu_{0.06}Be_{0.126})_{100-x}Fe_x$ (x=0, 2) BMGCs, continuous isothermal treatments at 600 K were conducted in DMA tests. During the isothermal treatment, both specimens were firstly heated to 600 K (below the glass transition temperature) and then annealed for 12 h. Then, the annealed specimens were reheated from ambient temperature to 853 K under frequency of 1 Hz and heating rate of 3 K/min. As shown in Fig. 5, the physical aging treatment below the glass transition temperature induces the decrease in loss factor tanδ for Fe2 BMGC. The red fitting curve is obtained through Kohlrausch-Williams-Watts (KWW) equation. The trends reflect the structural relaxation in the metallic glass forming liquids, leading to the decrease in viscoelastic component and the increase in elastic component[54].

Physical aging is an effective method to observe defects in metallic glasses, such as free volume[55], soft-zone defects[56–57], and quasi-point defects[58], which correspond to the fluctuations of density, entropy, and enthalpy, respectively. These theories are related to the structural heterogeneity and atomic mobility in the metallic glasses. Physical aging causes a non-exponential decline in loss factor tanδ, which can be well fitted by KWW equation or stretched exponential decay function[59], as follows:

$$\tan\delta(t)-\tan\delta(t=\infty)=A\exp\left[-\left(\frac{t}{\tau}\right)^{\beta_{KWW}}\right] \quad 0<\beta_{KWW}\leqslant 1 \quad (1)$$

where t is aging time; τ is the characteristic relaxation time; A is the maximum magnitude of decay with A=tan$\delta(t=0)$ − tan$\delta(t=\infty)$; β_{KWW} is the stretched exponential parameter of 0–1, reflecting the deviation extent of the single Debye relaxation and the broad distribution of relaxation time. Eq.(1) equals the single Debye relaxation time when β_{KWW} = 1. As for the metallic glasses, β_{KWW} is closely related to the structural heterogeneity. Usually, the stretched exponent β_{KWW} of metallic glasses is close to 0.5[60–61]. Considering the evolution of loss factor tanδ, the parameter Δ is defined as a function of aging time t, as follows:

$$\Delta=\frac{\tan\delta(t)-\tan\delta(t=\infty)}{\tan\delta(t=0)-\tan\delta(t=\infty)} \quad (2)$$

where $\tan\delta(t=\infty)$ and $\tan\delta(t=0)-\tan\delta(t=\infty)$ can be directly obtained from the fitting results of Eq.(1). As shown in Fig. 5, β_{KWW} value is 0.36. The insert in Fig. 5 shows the relationship between ln[−ln(Δ)] and ln$t$, and the slope of fitting line is close to the stretched exponent β_{KWW}.

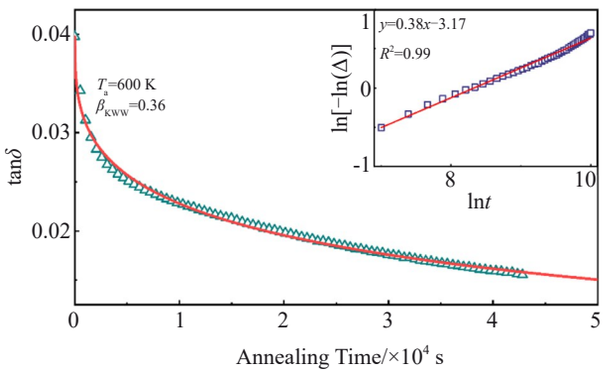

Fig.5 Relationship between loss factor tanδ and annealing time of Fe2 BMGC (inset shows the relationship between ln[−ln(Δ)] and ln$t$)

In order to further analyze the influence of physical aging on microstructural properties of Fe0 and Fe2 BMGCs, four specimens were prepared for XRD and DSC tests: the specimens were heated to 600 K and annealed for 12 h. Fig. 6 shows XRD patterns of Fe0 and Fe2 BMGCs after heating to 600 K and annealing at 600 K for 12 h. It can be seen that after annealing treatment, the Bragg peaks of β-Ti become more obvious, which indicates the precipitation of dendrites. After annealing at 600 K for 12 h, ω-Ti phase can be detected, inferring the precipitation of ω-Ti from β-Ti during annealing process. This result explains the overshoot of storage modulus at about 600 K in DMA tests. The peak intensity reflects the volume fraction of β-Ti phase[20]. As shown in Fig. 6a and 6b,

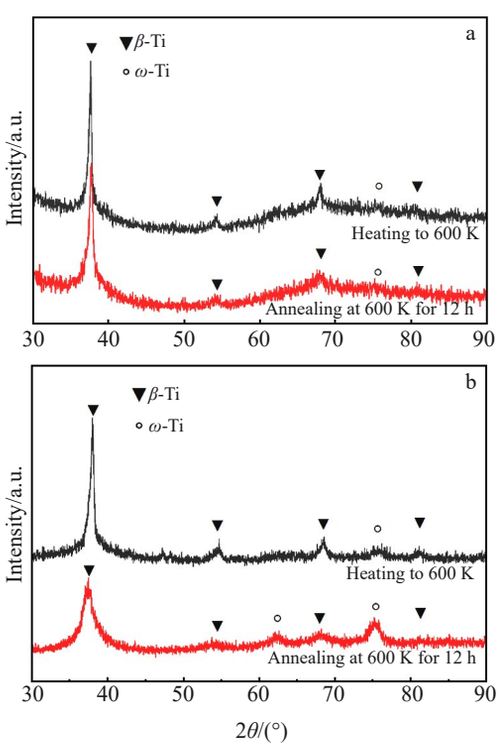

Fig.6 XRD patterns of Fe0 BMGC (a) and Fe2 BMGC (b) after heating to 600 K and annealing at 600 K for 12 h

the intensity of the first peaks slightly decreases, which is attributed to the phase transformation of β-Ti. Fig. 7 shows DSC curves of Fe0 and Fe2 BMGCs after heating to 600 K and annealing at 600 K for 12 h. It can be seen that the abnormal exothermic peaks at around 550 K of both BMGCs are negligible due to the irreversible phase transformation.

To investigate the effect of physical aging on structural relaxation, the as-annealed specimens were reheated to 853 K at the frequency of 1 Hz and heating rate of 3 K/min, as shown in Fig.8. After annealing at 600 K for 12 h, the storage modulus no longer shows the overshoot characteristic and the storage modulus of Fe0 and Fe2 BMGCs increases by about 50% and 40% at the low temperature range, respectively. The significant increase is attributed to the decrease in atomic mobility in the glassy matrix caused by annealing and the precipitation of ω phase from β-Ti crystalline phase. The loss modulus of Fe0 and Fe2 BMGCs is almost unchanged, and it decreases slightly around 500 K. However, the shoulder characteristic of Fe2 BMGC disappears, which is consistent with the above results. The shoulder phenomenon is irrelevant to the β relaxation but related to the phase transformation of β-Ti dendrites. Because β relaxation is the diffusion motion of the smallest constituent atom in metallic glasses, this process is reversible[62–63]. Hence, the irreversible shoulder phenomenon is ascribed to the precipitation of ω-Ti phase from the β-Ti crystalline. The ω phase has higher stacking density, compared with the bcc β-Ti[64], and the formation of ω phase leads to the decrease in atomic mobility. In addition, it can be concluded that the physical aging only affects the dynamic mechanical properties of BMGCs below the annealing temperature, and the dynamic complex moduli return to the modulus of the as-cast specimen when the temperature is above the annealing temperature, as shown in Fig.8.

Successive heating and cooling cycles were conducted to reveal the effects of thermal history on dynamic mechanical behavior. Fe2 BMGC was used as the test specimen. The target

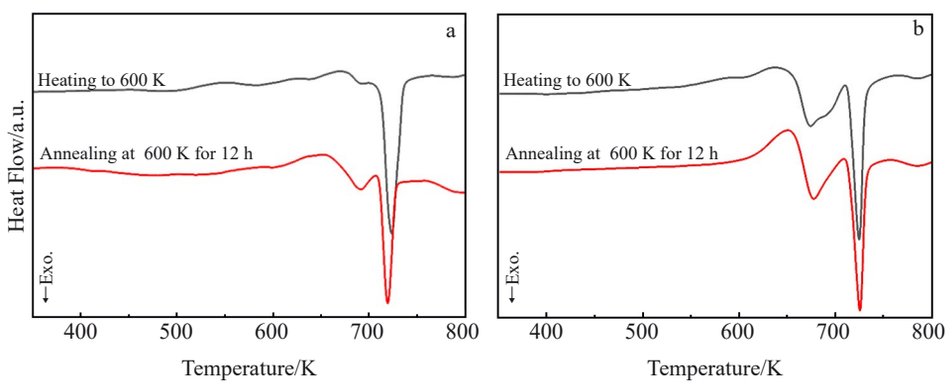

Fig.7 DSC curves of Fe0 BMGC (a) and Fe2 BMGC (b) after heating to 600 K and annealing at 600 K for 12 h at heating rate of 20 K/min

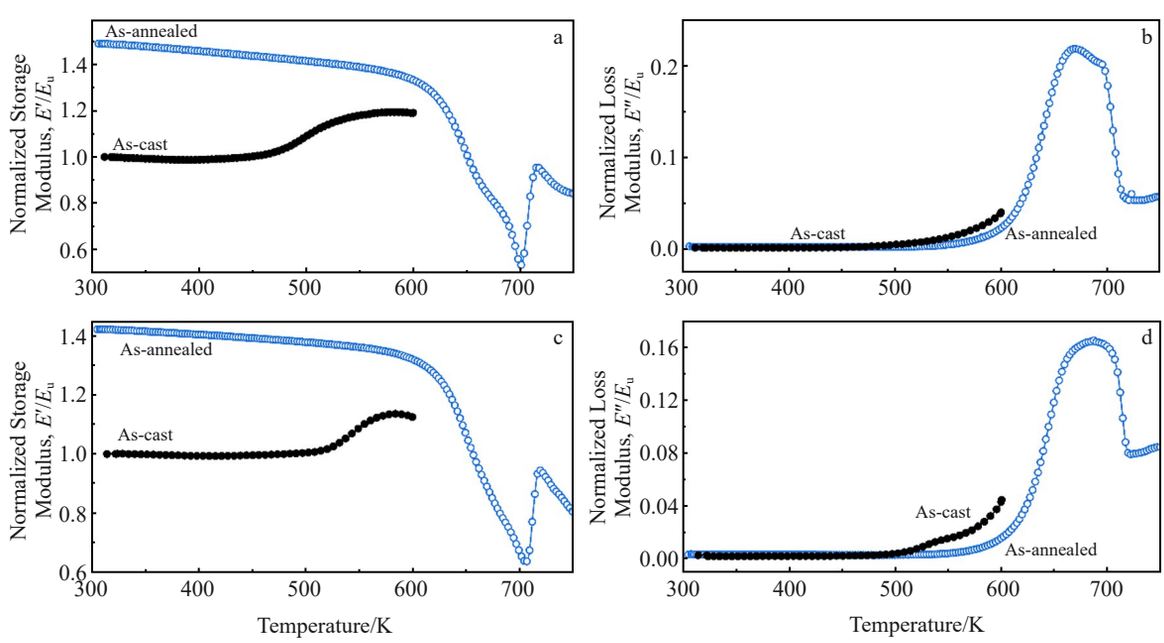

Fig.8 Normalized storage modulus E'/E_u (a, c) and normalized loss modulus E''/E_u (b, d) of as-cast and as-annealed Fe0 BMGC (a–b) and Fe2 BMGC (c–d)

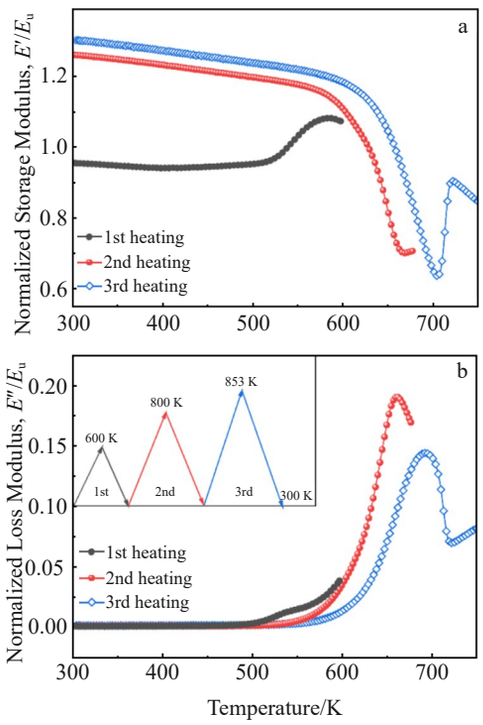

Fig.9 Normalized storage modulus E'/E_u (a) and normalized loss modulus E''/E_u (b) of Fe2 BMGC during continuous heating process at heating rate of 3 K/min and frequency of 1 Hz

temperature was 600, 680, and 853 K. As shown in Fig.9, the abnormal overshoot in the storage modulus vanishes after the first heating process to 600 K. In the first heating process, the loss modulus presents obvious shoulder characteristic. Then, the shoulder characteristic changes to the excess-wing characteristic in the second heating process. Finally, the characteristic disappears after the third heating to 680 K due to the irreversible structural changes, namely the precipitation of ω phase and the crystallization in glass matrix. After continuous heating, the glassy matrix is crystallized and the atomic mobility greatly decreases, indicating that the effect of thermal history is equal to that of annealing. Thus, the response of structural relaxation behavior changes. Briefly, the abnormal internal friction peak disappears after annealing below the glass transition temperature, which is probably caused by the fact that the metastable β phase changes to the phase at stable energy state under the excitation of thermal effects.

3 Conclusions

1) $(Ti_{0.474}Zr_{0.34}Cu_{0.06}Be_{0.126})_{100-x}Fe_x$ Ti-based bulk metallic glass composites (BMGCs) with x=0 and x=2 present the abnormal overshoot in storage modulus at around 500 and 550 K, respectively, which corresponds to the precipitation of ω-Ti phase in β-Ti dendrites.

2) Abnormal internal friction peaks appear in $(Ti_{0.474}Zr_{0.34}Cu_{0.06}Be_{0.126})_{98}Fe_2$ BMGC below the glass transition temperature, which correspond to the dendrites in composites to form a more stable long-period structure during the heating process.

3) The abnormal internal friction peak disappears after annealing below the glass transition temperature, which is probably caused by the fact that the metastable β phase changes to the phase at stable energy state under the excitation of thermal effects.

Acknowledgments: the authors thank Dr. Zhang Long from Institute of Metal Research, Chinese Academy of Sciences for provision of samples.

References

1 Wang W H. *Progress in Materials Science*[J], 2012, 57(3): 487
2 Sun B A, Song K K, Pauly S *et al. International Journal of Plasticity*[J], 2016, 85: 34
3 Lei Yang, Wang Pei, Deng Liang *et al. Rare Metal Materials and Engineering*[J], 2022, 51(4): 1497 (in Chinese)
4 Zheng X W, Zhou Y Y, Chu Z H *et al. Rare Metal Materials and Engineering*[J], 2020, 49(9): 2978
5 Zhang B Y. *Rare Metal Materials and Engineering*[J], 2016, 45(11): 2818
6 Yuan Zizhou, Yao Lin, Bao Shilei *et al. Rare Metal Materials and Engineering*[J], 2009, 38(6): 999 (in Chinese)
7 Greer A L, Cheng Y Q, Ma E. *Materials Science and Engineering R: Reports*[J], 2013, 74(4): 71
8 Liu Y Y, Liu P Z, Li J J *et al. International Journal of Plasticity*[J], 2018, 105: 225
9 Eckert J, Das J, Pauly S *et al. Journal of Materials Research*[J], 2007, 22(2): 285
10 Sun B A, Wang W H *et al. Progress in Materials Science*[J], 2015, 74: 211
11 Lee M L, Li Y, Schuh C A. *Acta Materialia*[J], 2004, 52(14): 4121
12 Choi-Yim H, Busch R, Köster U *et al. Acta Materialia*[J], 1999, 47(8): 2455
13 Hofmann D C, Suh J Y, Wiest A *et al. Proceedings of the National Academy of Sciences*[J], 2008, 105(51): 20136
14 Ma Yunfei, Gong Pan, Li Fangwei *et al. Rare Metal Materials and Engineering*[J], 2020, 49(4): 1445 (in Chinese)
15 Jiang F, Chen G, Wang Z H *et al. Rare Metal Materials and Engineering*[J], 2011, 40(2): 206
16 Qiu Keqiang, Ren Yinglei. *Rare Metal Materials and Engineering*[J], 2006, 35(1): 66 (in Chinese)
17 Chu Zhenhua, Yuan Guangyin, Hidemi Kato *et al. Rare Metal Materials and Engineering*[J], 2013, 42(6): 1154 (in Chinese)
18 Pan D G, Zhang H F, Wang A M *et al. Applied Physics Letters*[J], 2006, 89: 261904
19 Conner R D, Dandliker R B, Scruggs V *et al. International Journal of Impact Engineering*[J], 2000, 24(5): 435
20 Qiao J W, Jia H, Liaw P K. *Materials Science and Engineering R: Reports*[J], 2016, 100: 1
21 Du X H, Huang J C, Hsieh K C *et al. Applied Physics Letters*[J], 2007, 91: 131901
22 Wu Y, Xiao Y H, Chen G L *et al. Advanced Materials*[J], 2010, 22(25): 2770
23 Qiao J W, Sun A C, Huang E W *et al. Acta Materialia*[J], 2011,

59(10): 4126
24 Guo Zhenxi, Wang Yongsheng, Sui Manling *et al. Rare Metal Materials and Engineering*[J], 2017, 46(9): 2558 (in Chinese)
25 Hofmann D C, Suh J Y, Wiest A *et al. Nature*[J], 2008, 451(7182): 1085
26 Oh Y S, Kim C P, Lee S *et al. Acta Materialia*[J], 2011, 59(19): 7277
27 Cytron S J. *Journal of Materials Science Letters*[J], 1982, 1(5): 211
28 Scudino S, Liu G, Prashanth K G *et al. Acta Materialia*[J], 2009, 57(6): 2029
29 Jeon C, Kim C P, Joo S H *et al. Acta Materialia*[J], 2013, 61(8): 3012
30 Zhang L, Zhang J H, Ke H B *et al. Acta Materialia*[J], 2022, 222: 117444
31 Wu Xiaofeng, Zhang Guangan, Wu Fufa. *Rare Metal Materials and Engineering*[J], 2017, 46(4): 1086 (in Chinese)
32 Wu Y, Wang H, Wu H H *et al. Acta Materialia*[J], 2011, 59(8): 2928
33 Pauly S, Liu G, Wang G *et al. Acta Materialia*[J], 2009, 57(18): 5445
34 Liu Z Q, Li R, Liu G *et al. Acta Materialia*[J], 2012, 60(6–7): 3128
35 Wu Y, Zhou D Q, Song W L *et al. Physical Review Letters*[J], 2012, 109: 245506
36 Fornell J, Concustell A, Suriñach S *et al. International Journal of Plasticity*[J], 2009, 25(8): 1540
37 Jiang J Z, Hofmann D, Jarvis D J *et al. Advanced Engineering Materials*[J], 2015, 17(6): 761
38 Qiao J W, Jia H L, Zhang Y *et al. Materials Chemistry and Physics*[J], 2012, 136(1): 75
39 Zhao Yanchun, Mao Ruipeng, Xu Congyu *et al. Rare Metal Materials and Engineering*[J], 2019, 48(6): 1841 (in Chinese)
40 Zhang L, Zhu Z W, Fu H M *et al. Materials Science and Engineering A*[J], 2017, 689: 404
41 Cui J, Liu X, Liu Y. *Rare Metal Materials and Engineering*[J], 2022, 51(5): 1637
42 Kolodziejska J A, Kozachkov H, Kranjc K *et al. Scientific Reports*[J], 2016, 6(1): 22563
43 Qiao J C, Pelletier J M, Kou H C *et al. Intermetallics*[J], 2012, 28: 128
44 Qiao J C, Sun B A, Gu J *et al. Journal of Alloys and Compounds*[J], 2017, 724: 921
45 Lyu G J, Qiao J C, Pelletier J M *et al. Journal of Alloys and Compounds*[J], 2020, 819: 153040
46 Qiao J C, Ren T P, Lyu G J *et al. Materials Science and Engineering A*[J], 2019, 739: 193
47 Qiao J C, Pelletier J M, Casalini R. *Journal of Physical Chemistry B*[J], 2013, 117: 13658
48 Zhang L, Chen S, Fu H M *et al. Materials and Design*[J], 2017, 133: 82
49 Petry W. *Phase Transitions*[J], 1991, 31(1–4): 119
50 Caillard D, Martin J L. *MRS Bulletin*[J], 2003, 30: 319
51 Qiao J C, Wang Q, Pelletier J M *et al. Intermetallics*[J], 2018, 102: 6
52 Gallino I, Cangialosi D, Evenson Z *et al. Acta Materialia*[J], 2018, 144: 400
53 Sun Y, Peng S X, Yang Q *et al. Physical Review Letters*[J], 2019, 123(10): 105701
54 Wang W H. *Progress in Materials Science*[J], 2019, 106: 100561
55 Spaepen F. *Acta Metallurgica*[J], 1977, 25(4): 407
56 Li W D, Gao Y F, Bei H B. *Scientific Reports*[J], 2015, 5(1): 14786
57 Li W, Bei H, Tong Y *et al. Applied Physics Letters*[J], 2013, 103(17): 171910
58 Wang Q, Pelletier J M, Dong Y D *et al. Materials Science and Engineering A*[J], 2004, 379(1–2): 197
59 Hiki Y, Tanahashi M, Takeuchi S. *Journal of Non-crystalline Solids*[J], 2008, 354(10–11): 994
60 Shimshoni E, Gefen Y. *Annals of Physics*[J], 1991, 210(1): 16
61 Qiao J C, Zhang L T, Tong Y *et al. Advances in Mechanics*[J], 2022, 52(1): 117 (in Chinese)
62 Duan Y J, Zhang L T, Qiao J C *et al. Physical Review Letters*[J], 2022, 129: 175501
63 Liang S Y, Zhang L T, Wang B *et al. Intermetallics*[J], 2024, 164: 108115
64 Banerjee S, Tewari R, Dey G K. *International Journal of Materials Research*[J], 2006, 97(7): 963

内生型$(Ti_{0.474}Zr_{0.34}Cu_{0.06}Be_{0.126})_{100-x}Fe_x$ (x=0, 2)金属玻璃基复合材料的动态力学行为

肖海洋，吕国建，乔吉超
(西北工业大学 力学与土木建筑学院，陕西 西安 710072)

摘 要： 为了解内生β-Ti相的Zr/Ti基金属玻璃复合材料的动态力学性能和热力学稳定性，采用力学弛豫谱研究了$(Ti_{0.474}Zr_{0.34}Cu_{0.06}Be_{0.126})_{100-x}Fe_x$（$x$=0，2）金属玻璃复合材料。通过引入Fe元素，提高了β-Ti相的稳定性。此外，还发现了一个异常的内耗峰，这是由于在亚稳的β-Ti相中析出ω-Ti所引起的。在玻璃化转变温度T_g以下，由于相变和非晶基体部分结晶的耦合效应，2种金属玻璃复合材料的储能模量均表现出异常过冲行为。所得结果为更好地理解内生亚稳β-Ti型金属玻璃复合材料的复杂动态力学弛豫行为提供了借鉴。

关键词： 块体金属玻璃复合材料；动态力学分析；物理时效；动态非均匀性

作者简介：肖海洋，女，1999年生，硕士，西北工业大学力学与土木建筑学院，陕西 西安 710072，电话：029-88431000，E-mail：xiaohy@mail.nwpu.edu.cn